TOPOLOGY OPTIMIZATION FOR MINIMUM STRESS DESIGN WITH THE HOMOGENIZATION METHOD

Grégoire ALLAIRE, François JOUVE,
Centre de Mathématiques Appliquées (UMR 7641), Ecole Polytechnique,
91128 Palaiseau, France
and Hervé MAILLOT
Laboratoire MAPMO (UMR 6628), Université d'Orléans
B.P. 6759, 45067 Orléans cedex, France

3 juillet 2003

Résumé

This paper is devoted to minimum stress design in structural optimization. The homogenization method is extended to such a framework and yields an efficient numerical algorithm for topology optimization. The main idea is to use a partial relaxation of the problem obtained by introducing special microstructures which are sequential laminated composites. Indeed, the so-called corrector terms of such microgeometries are explicitly known, which allow us to compute the relaxed objective function. These correctors can be interpreted as stress amplification factors, caused by the underlying microstructure.

1 Introduction

The homogenization method for topology optimization in structural design is by now well established (see the books [1], [7], [12], or the numerical works [4], [6], [8], and references therein). However, the theory, as well as the numerical practice, is mostly restricted to compliance, eigenfrequency or displacement field optimization (in the single or multiple loadings case). The main problem is that optimal microstructures (which are crucial in the derivation of the relaxed objective function) are known only for special objective functions, all related to the stored elastic energy. This difficulty can be alleviated (at least from a numerical point of view) by working with a subclass of microstructures, possibly suboptimal but fully explicit. The simplest class is that of sequential laminated composites which have fully explicit homogenized properties. This approach has been followed in [2], [5] (see also Section 5.2.8 in [1]) and is called a partial relaxation of the problem.

The goal of this paper is to extend, from a numerical point of view, the homogenization method to another type of objective functions corresponding to minimum stress design. A typical example of such objective functions is

$$\inf_{\Omega} \int_{\Omega} |\sigma|^2 \, dx, \tag{1}$$

where σ is the stress tensor in the elastic body Ω. There are already some theoretical works that studied the relaxation of (1), either in the present elasticity context or in conductivity, [15], [18], [24], [26], but they do not furnish a fully explicit framework for numerical computations. On the other hand, some papers, including [14], [17], already provided numerical algorithms for some special type of microstructures. The present paper pertains to the latter category. We introduce a partial relaxation of the problem based on the use of laminated microstructures. Compared to the usual homogenization method, an additional difficulty arises which is due to the microscopic fluctuations of the stress tensor. Indeed, it is well-known that microscopic heterogeneities may cause stress concentrations, so that the actual stress distribution is very different from the macroscopic averaged stress. In the vocabulary of homogenization theory, the previous mechanical statement can be phrased as : when the size ϵ of the heterogeneities go to zero, the stress tensor σ_ϵ converges weakly (or in average) to the homogenized stress σ but not strongly or pointwise. Therefore, when extending the objective function (1) to composite materials (as does the homogenization method), one must multiply the macroscopic stress tensor by a stress amplification factor which takes into account the microscopic heterogeneities. In other words, the relaxed or homogenized objective function is

$$\inf_{\Omega} \int_{\Omega} |\mathcal{P}\sigma|^2 \, dx, \tag{2}$$

where the tensor $\mathcal{P} \geq \mathrm{Id}$ can be computed in terms of so-called corrector terms. For general microstructures, it is very difficult to compute these correctors. However, for laminated composite materials, there exists an explicit formula of the correctors (this is a classical result in mechanics [20] but a rigorous proof is due to Briane [11]).

Note that there are many generalizations of the homogenization method which avoids the use of the full theory of homogenization. Let us quote, for example, the convexification method, fictitious or power-law materials (also called SIMP method, see e.g. [7], [9], [25], [10], [27]). However, even for such simplified heuristic methods, the problem of taking into account the microscopic stress concentrations has to be solved if one wants a clear mechanical interpretation of the generalized objective function.

Finally let us make a brief comparison between our work and that of Bendsoe and Duysinx [14]. In both cases a local stress field is reconstructed which is different from the averaged macroscopic stress (computed by a finite element method) and the minimal stress criterion is evaluated with this local stress (and not the average one). However, we emphasize two major differences between the approach followed by Bendsoe and Duysinx and ours. They used a pointwise maximum stress criteria wheras we work with the simpler and smoother L^2-norm critera (2). Although we can localize this criterion in a subdomain (see the numerical examples in Section 6), it is clear that our choice of the L^2-norm critera is less sound from a mechanical point of view. On the other hand, they were limited to orthogonal rank-two laminates while we can compute the stress amplification factor $\mathcal{P}$ for sequential laminates of any rank. Clearly, our class of microstructures being much larger, we can find among them better (near optimal ?) microstructures for minimizing the local stress criterion.

The content of the paper is the following. In Section 2 the problem of minimum stress design is introduced in the classical setting of shape optimization. Section 3 is devoted to recalling some useful results of homogenization theory and proposes a partial relaxation of the problem. Section 4 focuses on the computation of the correctors (or stress amplification factors) in the case of laminated composite materials. Section 5 gives the details of the proposed partial relaxation and numerical algorithm. Finally Section 6 is concerned with numerical examples.

2 Setting of the problem

Although our main motivation is shape optimization (i.e. punching holes in a given material B), we formulate the problem as a two-phase optimization problem involving a strong material B and a weak one A, mimicking holes. This is common practice in the homogenization method for shape optimization and it has the advantage of avoiding many technical difficulties. Shape optimization corresponds to the degenerate limit $A \to 0$, but we shall not try to justify it rigorously.

We consider a bounded domain $\Omega \in \mathbb{R}^N$, with $N = 2$ or 3, occupied by two linearly elastic isotropic phases A and B. Their Hooke's laws, also denoted by A and B, are given for any symmetric matrix ξ by

$$A\xi = 2\mu_A \xi + \left(\kappa_A - \frac{2\mu_A}{N}\right)(\mathrm{tr}\xi)\, I_2, \quad B\xi = 2\mu_B \xi + \left(\kappa_B - \frac{2\mu_B}{N}\right)(\mathrm{tr}\xi)\, I_2,$$

where $0 < \mu_A < \mu_B$ are the shear moduli and $0 < \kappa_A < \kappa_B$ are the bulk moduli. It is convenient to introduce a Lamé coefficient, proportional to the Poisson's ratio, defined by

$$\lambda_A = \kappa_A - \frac{2\mu_A}{N}, \quad \lambda_B = \kappa_B - \frac{2\mu_B}{N}.$$

Let $\chi \in L^\infty(\Omega; \{0,1\})$ be the characteristic function of phase A (i.e. taking the value 1 in A and 0 outside). We define an overall Hooke's law in Ω by

$$A_\chi(x) = \chi(x)A + (1 - \chi(x))B.$$

The corresponding displacement u_χ of this structure is computed as the unique solution in $H^1_0(\Omega)^N$ of

$$\left\{ \begin{array}{ll} \sigma_\chi = A_\chi e(u_\chi) & \text{in } \Omega \\ -\,\mathrm{div}\sigma_\chi = f & \text{in } \Omega \\ u_\chi = 0 & \text{on } \partial\Omega, \end{array} \right. \tag{3}$$

where $e(u_\chi) = (\nabla u + \nabla^t u)/2$ is the strain tensor, and f is a given body force in $L^2(\Omega)^N$.

For simplicity, we work with a model problem having Dirichlet boundary conditions, but clearly more general surface loadings or boundary conditions are allowed. We address the following two-phase optimal design problem

$$\inf_{\chi \in L^\infty(\Omega;\{0,1\})} J(\chi), \tag{4}$$

with an objective function J defined by

$$J(\chi) = \int_\Omega k(x)|\sigma_\chi|^2 dx, \tag{5}$$

where $k(x)$ is a given piecewise smooth non-negative function (a weighting factor that can localize the objective function). More generally we can set

$$J(\chi) = \int_\Omega j(x, \sigma_\chi) dx,$$

with a smooth function j with quadratic growth in σ. This allows us, for example, to minimize the equivalent Von Mises stress intensity in Ω. Similarly, we could consider a function $j(x, e(u_\chi))$ depending on the strain tensor.

In general, (4) is expected to be an ill-posed problem which requires relaxation, i.e. for which there exist only generalized optimal solutions (see e.g. [1], [15], [16], [22], [18], [24], [26]). These generalized designs are defined as composite materials obtained by mixing on a microscopic scale the two phases A and B. Such composite materials can be mathematically described thanks to homogenization theory.

3 Homogenization and partial relaxation.

We begin by recalling some basic facts from homogenization theory. Let χ_ϵ be a sequence of characteristic functions in $L^\infty(\Omega; \{0,1\})$ (for example, a minimizing sequence for the optimal design problem (4)). The main result of homogenization theory ([21], or Theorem 1.2.16 of [1]) tells us that, up to a subsequence still indexed by ϵ, the following convergences hold

$$\begin{aligned} \chi_\epsilon &\rightharpoonup \theta \text{ weakly-* in } L^\infty(\Omega; [0,1]), \\ A_\epsilon = \chi_\epsilon A + (1-\chi_\epsilon) B &\overset{\text{H}}{\rightharpoonup} A^* \text{ in the sense of homogenization.} \end{aligned} \tag{6}$$

where (θ, A^*) parameterizes a composite material with proportion $0 \leq \theta \leq 1$ of phase A and homogenized elasticity tensor A^* (corresponding to the microstructure or geometric arrangement of the two phases). As a consequence, the sequence of displacements u_ϵ (solution of (3) with the characteristic function χ_ϵ) satisfy

$$\begin{aligned} u_\epsilon &\rightharpoonup u \text{ weakly in } H_0^1(\Omega)^N, \\ \sigma_\epsilon = A_\epsilon e(u_\epsilon) &\rightharpoonup \sigma \text{ weakly in } L^2(\Omega, \mathbb{R}^{N^2}), \end{aligned} \tag{7}$$

where u is the homogenized displacement, and σ the homogenized stress, solutions of the relaxed state equation

$$\begin{cases} \sigma = A^* e(u) & \text{in } \Omega, \\ -\operatorname{div}\sigma = f & \text{in } \Omega, \\ u = 0 & \text{on } \partial\Omega. \end{cases} \tag{8}$$

Unfortunately, the weak convergence in (7) does not allow to pass to the limit in the objective function (5). In general, we have

$$\liminf_{\epsilon\to 0}\int_\Omega k(x)|\sigma_\epsilon|^2dx \ge \int_\Omega k(x)|\sigma|^2dx,$$

where the inequality is strict for most sequences. This is in sharp contrast with all other previous applications of the homogenization method for which usually the objective function does not depend on the stress nor on the strain (as, for example, compliance, eigenfrequency, or a least-square criterion of approximation of a target displacement).

In order to pass to the limit in the objective function (5), and thus to determine the relaxed formulation of (4), we need to have a strong convergence result instead of the weak one in (7). This can be obtained by introducing so-called correctors terms. Homogenization theory ([21], or Section 1.3.6 of [1]) states that there exist a sequence W_ϵ of fourth-order tensors (called correctors) which satisfy

$$\begin{array}{rcl} W_\epsilon & \rightharpoonup & I_4 \text{ weakly in } L^2(\Omega, \mathbb{R}^{N^4}), \\ A_\epsilon W_\epsilon & \rightharpoonup & A^* \text{ weakly in } L^2(\Omega, \mathbb{R}^{N^4}), \\ (W_\epsilon)^t A_\epsilon W_\epsilon & \rightharpoonup & A^* \text{ weakly in } L^1(\Omega, \mathbb{R}^{N^4}), \end{array} \tag{9}$$

where I_4 is the fourth-order identity tensor. The main interest of the corrector tensor W_ϵ is that it corrects the lack of pointwise convergence of the strain and stress tensors, namely

$$\begin{array}{rcl} e(u_\epsilon) - W_\epsilon e(u) & \to & 0 \text{ strongly in } L^1(\Omega, \mathbb{R}^{N^2}), \\ \sigma_\epsilon - A_\epsilon W_\epsilon {A^*}^{-1}\sigma & \to & 0 \text{ strongly in } L^1(\Omega, \mathbb{R}^{N^2}). \end{array} \tag{10}$$

In the sequel, we shall use the notation $P_\epsilon = A_\epsilon W_\epsilon {A^*}^{-1}$ which is a sequence of tensors converging weakly to I_4 in $L^2(\Omega, \mathbb{R}^{N^4})$. The main idea is now to rewrite the objective function as

$$J(\chi_\epsilon) = \int_\Omega k(x)|P_\epsilon\sigma|^2dx + r_\epsilon, \tag{11}$$

with a (hopefully) small remainder term

$$r_\epsilon = \int_\Omega k(x)\left(\sigma_\epsilon - P_\epsilon\sigma\right)\cdot\left(\sigma_\epsilon + P_\epsilon\sigma\right)dx.$$

If one can prove that $\lim_{\epsilon\to 0} r_\epsilon = 0$, then we obtain the desired result

$$\lim_{\epsilon\to 0} J(\chi_\epsilon) = \int_\Omega k(x)|\mathcal{P}\sigma|^2dx, \tag{12}$$

where $\mathcal{P}^2$ is the weak limit of P_ϵ^2. Since P_ϵ converges weakly to I_4, we have the following estimate (in the sense of quadratic forms)

$$\mathcal{P} \ge I_4, \tag{13}$$

which justifies our terminology of **stress amplification factor** for this tensor $\mathcal{P}$. (Note that Lipton [17] wrote $|\mathcal{P}\sigma|^2 = |\sigma|^2 + S\sigma\cdot\sigma$ and called S the covariance tensor.)

Remark 3.1. *Remark that the convergences in (10) hold in the space* $L^1(\Omega, \mathbb{R}^{N^2})$ *and not in* $L^2(\Omega, \mathbb{R}^{N^2})$ *as is required to prove that* $\lim_{\epsilon\to 0} r_\epsilon = 0$. *The reason is that, in general,* W_ϵ *and* ∇u *are merely* L^2 *functions, so their product belongs only to* L^1.

Thanks to a regularity result of Meyers [23] (see Theorem 1.3.41 of [1] for its application in the context of homogenization), one can improve slightly the convergences in (10). Indeed, let $p > 2$ *be the Meyers exponent, i.e. the largest exponent such that the gradients of the solutions of (3) or (8) belong to* $L^p(\Omega)$. *(Such an exponent does exist and depends only on* A *and* B *which are lower and upper bounds for any elasticity tensor* A_χ *or* A^* *involved in the above partial differential equations.) Then, convergences in (10) hold in the space* $L^q(\Omega, \mathbb{R}^{N^2})$ *with* $q = min(2, p/2) > 1$ *(see Corollary 1.3.43 of [1]). It may still happen that* $q < 2$ *and thus this improved convergence is not enough to prove that* $\lim_{\epsilon\to 0} r_\epsilon = 0$. *In such a case, the best that we can hope is to pass to the limit in a objective function similar to (11) but with the exponent* $q < 2$.

We are not able to prove (12) for any sequence of characteristic functions χ_ϵ (i.e. for any type of composite materials). Even if we could, the consequences of such a result would be of limited practical interest since the stress amplification factor $\mathcal{P}$ is not explicitly computable in most instances. This is the reason why we restrict ourselves to a special class of composites, namely the **sequential laminated composites**. A sequential laminate is defined by iteratively layering the two phases A and B in different directions and proportions and at well-separated lengthscales. A laminate is said to have core A and matrix B when phase A is used only at the first layering iteration (at smallest lengthscale) and only B is layered with the previously obtained laminate at the next iterations (see Figure 1 for an example, and [1], [20] for further details).

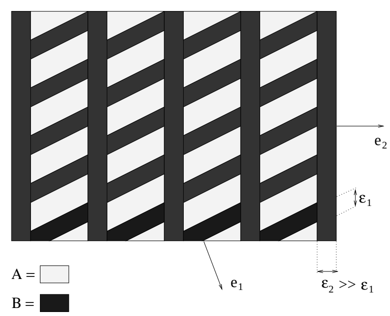

FIG. 1 – A rank-2 sequential laminate with core A and matrix B.

A sequential laminate A^*, with core A and matrix B, in proportions θ and $(1-\theta)$ respectively, is characterized by its lamination directions $(e_i)_{1\le i\le q}$ (unit vectors of $\mathbb{R}^N$) and its lamination parameters $(m_i)_{1\le i\le q}$, satisfying $m_i \ge 0$ and $\sum_{i=1}^q m_i = 1$. Its Hooke's law is explicitly given by

$$\theta\,(A^* - B)^{-1} \;=\; (A-B)^{-1} + (1-\theta)\sum_{i=1}^{q} m_i f_B(e_i), \tag{14}$$

where $f_B(e)$ is defined by

$$f_B(e)\xi : \xi = \frac{1}{\mu_B}\left(|\xi e|^2 - (\xi e\cdot e)^2\right) + \frac{1}{2\mu_B + \lambda_B}(\xi e\cdot e)^2. \tag{15}$$

Furthermore, there also exists an explicit formula for the corrector P_ϵ and the stress intensity factor $\mathcal{P}$ of such sequential laminates (see Section 4 below). In particular, $\mathcal{P}$, as A^*, depends only the parameters θ, $(e_i)_{1\le i\le q}$ and $(m_i)_{1\le i\le q}$. The set of all Hooke's laws A^* given by (14) and corresponding $\mathcal{P}$ (with the same parameters) is denoted by AP_θ.

As a final ingredient, we recall here one of the results of Briane [11] concerning correctors for laminated composites.

Lemma 3.2 (Briane). *For any laminated composite, there exist corrector tensors W_ϵ and P_ϵ, satisfying (9) and (10), which furthermore are uniformly bounded in $L^\infty(\Omega, \mathbb{R}^{N^4})$.*

By using Lemma 3.2, we can improve the convergences in (10), as is stated in the next result.

Proposition 3.3. *Let χ_ϵ be a sequence of characteristic functions corresponding to a laminated composite. Let W_ϵ and P_ϵ be the corrector tensors, belonging to $L^\infty(\Omega, \mathbb{R}^{N^4})$ by Lemma 3.2. Then, the convergence (10) holds true in $L^2(\Omega, \mathbb{R}^{N^2})$ and the desired convergence (12) of the objective function holds true.*

Proof. This is a simple adaptation of the classical proof of (10) due to Murat and Tartar [21] (see also Corollary 1.3.43 of [1]). This classical argument shows that, if u_n is a sequence of smooth functions that converges strongly to u in $H_0^1(\Omega)^N$, then

$$\lim_{\epsilon\to 0} \|e(u_\epsilon) - W^\epsilon e(u_n)\|^2_{L^2(\Omega)} \le C\|e(u) - e(u_n)\|^2_{L^2(\Omega)}.$$

On the other hand, we have the following estimate

$$\begin{aligned}
\|e(u_\epsilon) - W^\epsilon e(u)\|_{L^2(\Omega)} &\le \|e(u_\epsilon) - W^\epsilon e(u_n)\|_{L^2(\Omega)} \\
&\quad + \|W^\epsilon\|_{L^\infty(\Omega)} \|e(u-u_n)\|_{L^2(\Omega)} \\
&\le C\left(\|e(u_\epsilon) - W^\epsilon e(u_n)\|_{L^2(\Omega)} + \|e(u-u_n)\|_{L^2(\Omega)}\right).
\end{aligned}$$

Combining these two inequalities and letting n go to infinity, we obtain the desired convergence (10) in $L^2(\Omega, \mathbb{R}^{N^2})$ instead of merely $L^1(\Omega, \mathbb{R}^{N^2})$. This obviously implies $\lim_{\epsilon\to 0} r_\epsilon = 0$, and thus (12) holds true. □

Remark 3.4. *All corrector results are stated in the space $L^2(\Omega)$. It is easily seen on some explicit examples that the corrector tensors W_ϵ and P_ϵ are not enough to obtain strong convergence in spaces $L^p(\Omega)$ with $2 < p \le +\infty$. In other words, our computation of the local stress tensors (even for laminates) is complete only for an objective function of the type of (12). In general, there are other correctors terms which may be important in the L^∞-norm but which vanish in the L^2-norm. Therefore, we can not extend our approach to objective functions involving the maximum value of the stress.*

We are now in a position to propose a relaxed formulation of the original optimization problem (4). Once and for all we fix the set of lamination directions $(e_i)_{1\le i\le q}$ which are the same at every point in Ω. Then, we parameterize a sequential laminate design by a density function $\theta(x)$ and the lamination functions $(m_i(x))_{1\le i\le q}$ with values in the constraint set

$$\mathcal{M} = \left\{ m_i \ge 0 \text{ and } \sum_{i=1}^{q} m_i = 1 \right\}. \tag{16}$$

We define the set $\mathcal{LD}$ of sequentially laminated designs by

$$\mathcal{LD} = \{(\theta, m_i) \in L^\infty(\Omega; [0,1] \times \mathcal{M})\}. \tag{17}$$

For any design parameters $(\theta, m_i) \in \mathcal{LD}$ we can explicitly compute an homogenized tensor A^* by formula (14) and a stress amplification factor $\mathcal{P}$ by the formulas of section 4. The proposed partial relaxation is

$$\inf_{(\theta,m_i)\in\mathcal{LD}} \left\{ J^*(\theta, m_i) = \int_\Omega k(x)|\mathcal{P}\sigma|^2 dx \right\}, \tag{18}$$

where σ is the solution of (8).

Clearly, (18) is an extension of the original problem (4) since by taking $\theta = \chi$, a characteristic function, we obtain $A^* = A_\chi$ and $\mathcal{P} = I_4$, so we recover (4). Furthermore, any laminated design (θ, m_i) is attained as the limit (in the sense of homogenization as described above) of a sequence of classical designs $(\chi_\epsilon, A_\epsilon, P_\epsilon)$ with

$$J^*(\theta, m_i) = \lim_{\epsilon\to 0} J(\chi_\epsilon).$$

In particular, this implies that we have not changed the physical signification of the problem when passing from (4) to (18). Therefore, (18) is called a partial relaxation of (4). It is merely "partial" because we can not prove the existence of a solution to (18). However, if the class of sequential laminates is rich enough, (18) is a "more well-posed" minimization problem than (4). Numerically, we expect to have better properties (fast convergence, global minima) for the partial relaxation (18) since its integrand and its space of admissible designs have been smoothed or averaged, at least partially, leading to better convexity properties. As a possible justification of this partial relaxation (18), let us simply recall that in the cases of compliance or eigenfrequency optimization it coincides with the full relaxation.

As usual, a nearly optimal classical design can easily be recovered from an (almost) optimal composite design by a suitable penalization process. Of course, the main advantage of (18) is that it yields numerical algorithms that act as topology optimization methods.

4 Correctors for laminated composites.

In this section we describe the corrector associated to the homogenization a sequentially laminated composite with core A (the weak material) and matrix B. Briane [11] gave such an explicit corrector in a conductivity setting. His result was more general since any number of phases was allowed and the ordering of laminations was arbitrary. Here we simply rephrase his result in the elasticity case and for sequential laminates (we do not reproduce his proofs).

Let $e_1, ..., e_q$ be q unit vectors (lamination directions) in $\mathbb{R}^N$. For ϵ positive and arbitrarily small we define the Hooke's law of the rank-q laminate A_ϵ by

$$\begin{cases} A^1 & = A \\ A_\epsilon^{k+1} & = \chi_\epsilon^k B + (1 - \chi_\epsilon^k) A^k, \;\; 1 \le k \le q, \\ A_\epsilon^{q+1} & = A_\epsilon, \end{cases}$$

where $\chi_\epsilon^k(x) = \chi^k(\frac{x}{\epsilon^k})$ is the characteristic function of the k^{th} layer, with χ^k a $[0,1]^N$-periodic characteristic function and $\epsilon^k(\epsilon)$ a function going to zero with ϵ and satisfying an assumption of separation of scales, $\lim_{\epsilon\to 0} \epsilon^k(\epsilon)/\epsilon^{k+1}(\epsilon) = 0$ for $1 \leq k \leq q-1$ (the scale $k=1$ is thus the finest).

As is well-known in the mechanical literature (see e.g. [20]) and was first proved rigorously in [11], the strain tensor $e(u_\epsilon)$ in such a laminate is constant in each phase layer, up to a term strongly converging to zero in L^2. Hence, there exist $q+1$ constant matrices $\xi^1, ..., \xi^{q+1}$ (independent of ϵ) such that the strain tensor $e(u_\epsilon)$ can be obtained from the following induction formula (up to a term strongly converging to zero in L^2)

$$\left\{ \begin{array}{ll} \Xi_\epsilon^1 & = \xi^1, \\ \Xi_\epsilon^{k+1} & = \chi_\epsilon^k \xi^{k+1} + (1-\chi_\epsilon^k)\Xi_\epsilon^k, \ 1 \leq k \leq q, \\ \Xi_\epsilon^{q+1} & = e(u_\epsilon). \end{array} \right.$$

We explain below how to compute these constant tensors ξ_k. Before that, let us remark that a similar structure arises for the stress tensor $\sigma_\epsilon = A_\epsilon e(u_\epsilon)$ (again up to a term strongly converging to zero in L^2)

$$\left\{ \begin{array}{ll} \Sigma_\epsilon^1 & = A\xi^1, \\ \Sigma_\epsilon^{k+1} & = \chi_\epsilon^k B \xi^{k+1} + (1-\chi_\epsilon^k)\Sigma_\epsilon^k, \ 1 \leq k \leq q, \\ \Sigma_\epsilon^{q+1} & = \sigma_\epsilon. \end{array} \right.$$

As proved in [11], the corrector P_ϵ, introduced in (10), is defined similarly by

$$\left\{ \begin{array}{ll} C_\epsilon^1 & = P^1, \\ C_\epsilon^{k+1} & = \chi_\epsilon^k P^{k+1} + (1-\chi_\epsilon^k)C_\epsilon^k, \ 1 \leq k \leq q, \\ C_\epsilon^{q+1} & = P_\epsilon, \end{array} \right.$$

where the $q+1$ constant tensors P_k, $1 \leq k \leq q+1$, can be computed explicitly. Since $P_\epsilon\sigma - \sigma_\epsilon$ goes to zero in L^2, the above inductive definitions of σ_ϵ and P_ϵ leads to

$$P^1\sigma = A\xi^1, \ P^k\sigma = B\xi^k, \ 2 \leq k \leq q+1. \tag{19}$$

Using (19), we can now give a precise formula for the homogenized objective function $J^*(\theta, m_i)$. Let θ^k be the weak-$*$ limit of χ_ϵ^k. The quantity $|\mathcal{P}\sigma|^2$ is given by

$$\left\{ \begin{array}{ll} j^1 & = |A\xi^1|^2, \\ j^{k+1} & = \theta^k|B\xi^{k+1}|^2 + (1-\theta^k)j^k, \ 1 \leq k \leq q, \\ j^{q+1} & = |\mathcal{P}\sigma|^2. \end{array} \right.$$

An important feature of the above formula for the stress amplification factor $\mathcal{P}$ is its dependence with respect to the order of the lamination directions $(e_j)_{1\leq j\leq q}$. Indeed, enumerating these directions in a different order yields a different value of $\mathcal{P}$. This is in sharp contrast with the lamination formula (14) which delivers the value of the homogenized elasticity tensor A^* and which is independent of the ordering of the lamination directions.

Let us now explain how the strain tensors ξ_k, $1 \leq k \leq q+1$ are computed. Since the laminate is characterized by q separated scales (the first one being the smallest one), each heterogenous field representing the k first laminations can be seen, at the $(k+1)^{th}$ scale, as a homogeneous mean field. Let $\overline{\xi_{k+1}}$, $1 \leq k \leq q$, be the homogeneous mean strain tensor resulting from the k first laminations with the convention $\overline{\xi_1} = \xi_1$, $\overline{\xi_{q+1}} = e(u)$. We denote by A^*_k the rank-k laminate given by the following lamination formula

$$\left(1 - (1-\theta)\Sigma_{i=1}^{k} m_i\right)(A^*_k - B)^{-1} = (A-B)^{-1} + (1-\theta)\Sigma_{i=1}^{k} m_i f_B(e_i). \tag{20}$$

For every k, $1 \leq k \leq q$, we have

$$\overline{\xi_{k+1}} = \theta_k \xi_{k+1} + (1-\theta_k)\overline{\xi_k}. \tag{21}$$

>From the continuity of the displacement u at the interface between the regions occupied by A^*_{k-1} and B (this interface being a hyperplan normal to the vector e_k at scale k) we deduce the existence of a constant vector $w_k \in \mathbb{R}^N$ such that

$$\xi_{k+1} - \overline{\xi_k} = w_k \odot e_k = \frac{1}{2}\left(w_k \otimes e_k + e_k \otimes w_k\right). \tag{22}$$

Now let us note that the homogeneous mean stress resulting form the k first laminations and given by $A^*_k \overline{\xi_{k+1}}$, $1 \leq k \leq q$, is also equal to $\theta_k B \xi_{k+1} + (1-\theta_k) A^*_{k-1} \overline{\xi_k}$. After some tedious algebra we finally obtain

$$\xi_{k+1} = e(u) + (1-\theta_k) w_k \odot e_k - \sum_{i=k+1}^{q} \theta_i w_i \odot e_i, \tag{23}$$

with

$$w_k = q_k\left((A^*_{k-1} - B)\overline{\xi_{k+1}}\right) e_k, \tag{24}$$

where the symmetric matrix q_k is implicitly given by the following quadratic form

$$q_k^{-1} v \cdot v = \left((1-\theta_k)B + \theta_k A^*_{k-1}\right) v \odot e_k : v \odot e_k, \ \forall v \in \mathbb{R}^N. \tag{25}$$

5 Gradient algorithm for the partial relaxation

The advantage of dealing with generalized designs in $\mathcal{LD}$, instead of classical designs which are characteristic functions, is that we can easily compute the derivative of the objective function and build a gradient minimization algorithm. Recall that the lamination directions $(e_j)_{1 \leq j \leq q}$ are fixed (we assume that the unit sphere S_{N-1} is sufficiently discretized by these unit vectors). Thus the design parameters are the proportion $\theta(x)$ of phase A and the lamination parameters $\left(m_i(x)\right)_{1 \leq i \leq q}$.

For simplicity, the integrand of the objective function is considered as a function of $(x, e(u), \theta, m_i)$, which is always possible since $\sigma = A^*(\theta, m_i) e(u)$,

$$J^*(\theta, m_i) = \int_\Omega j(x, e(u), \theta, m_i)\, dx.$$

Note that, u also depends on θ and m_i, as the solution of (8). The objective function $J^*(\theta, m_i)$ is differentiable, and denoting by $\delta\theta$ and δm_i admissible increments, its directional derivative is

$$\delta J^*(\theta, m_i) = \int_\Omega \delta_\theta j \, \delta\theta \, dx + \sum_{i=1}^{q} \int_\Omega \delta_{m_i} j \, \delta m_i \, dx, \tag{26}$$

where

$$\begin{aligned} \delta_\theta j &= \frac{\partial j}{\partial \theta} + \frac{\partial j}{\partial u}\frac{\partial u}{\partial \theta}, \\ \delta_{m_i} j &= \frac{\partial j}{\partial m_i} + \frac{\partial j}{\partial u}\frac{\partial u}{\partial m_i}. \end{aligned} \tag{27}$$

In order to compute the above objective increments we introduce an adjoint state p solution of the equation (28) below and which allows to eliminate the partial derivatives of u in (27).

$$\begin{cases} -\operatorname{div}\left(A^* e(p)\right) = \frac{\partial j}{\partial u}(x, e(u), \theta, m_i) & \text{in } \Omega \\ p = 0 & \text{on } \partial\Omega. \end{cases} \tag{28}$$

Formally, the right hand side of (28) is

$$\frac{\partial j}{\partial u}(x, e(u), \theta, m_i) = -\operatorname{div}\left(\frac{\partial j}{\partial \xi}(x, \xi, \theta, m_i)\right) \quad \text{with} \quad \xi = e(u).$$

Indeed, we can rewrite $\delta_\theta j$ and $\delta_{m_i} j$ as follows :

$$\begin{aligned} \delta_\theta j &= \frac{\partial j}{\partial \theta} - \frac{\partial A^*}{\partial \theta} e(u) : e(p), \\ \delta_{m_i} j &= \frac{\partial j}{\partial m_i} - \frac{\partial A^*}{\partial m_i} e(u) : e(p), \end{aligned} \tag{29}$$

with the partial derivatives

$$\begin{aligned} \frac{\partial A^*}{\partial \theta} &= T^{-1}\left((A-B)^{-1} + \textstyle\sum_{i=1}^{q} m_i f_B(e_i)\right) T^{-1}, \\ \frac{\partial A^*}{\partial m_i} &= -\theta(1-\theta) T^{-1} f_B(e_i) T^{-1}, \\ T &= (A-B)^{-1} + (1-\theta) \textstyle\sum_{i=1}^{q} m_i f_B(e_i) \, . \end{aligned}$$

This gives the basis for a numerical gradient method which is described below. Of course, since (θ, m_i) are constrained locally at each point x (θ must stay in the range $[0,1]$, and the (m_i) must stay in the set $\mathcal{M}$ defined by (16)) the gradient method must be combined with a projection step to satisfy these constraints.

Remark 5.1. *For simplicity we focused on the case of a single load optimization problem. There is obviously no difficulty in extending the previous analysis to multiple load problems.*

We now have all the ingredients to define the proposed numerical algorithm.

1. Initialization of the design parameters θ_0, m_0 (for example, we take them constant satisfying the constraints).
2. Iteration until convergence, for $k \geq 0$:
   (a) Computation of the state u_k and the adjoint state p_k, solutions of (8) and (28) respectively, with the previous design parameters θ_k, m_k.
   (b) Updating of these parameters by

$$\begin{aligned}
\theta_{k+1} &= \max\left(0, \min\left(1, \theta_k - t_k \nabla_\theta J_k^*\right)\right), \\
m_{i,k+1} &= \max\left(0, m_{i,k} - t_k \nabla_{m_i} J_k^* + \ell_k\right).
\end{aligned}$$

   where ℓ_k is a Lagrange multiplier (iteratively adjusted) for the constraint $\sum_{i=1}^{q} m_{i,k} = 1$, and $t_k > 0$ is a small step such that

$$J^*(\theta_{k+1}, m_{k+1}) < J^*(\theta_k, m_k).$$

A good descent step t_k is computed through a line search that may be expensive since each evaluation of the objective function requires the solution of the direct and adjoint equation. In practice, we stop as soon as $J_{k+1}^* \leq J_k^*$ and we divide the step by two if not. Of course, more clever optimization schemes could be used.

6 Numerical results

We have tested our numerical method on various 2-D problems (see Figures 2 and 3; 3-D would work as well in principle) restricting ourselves to the following objective function :

$$J^*(\theta, m_i) = \int_\Omega j(x, e(u), \theta, m_i)dx = \int_\Omega \chi_\omega |\mathcal{P}\sigma|^2 dx, \tag{30}$$

where χ_ω is the characteristic function of a subset ω of the working domain Ω.

Remark 6.1. *Of course, the objective function (30) can easily be generalized, for instance, if one wants to minimize the equivalent Von Mises stress, by taking* $J^*(\theta, m_i) = \int_\Omega \chi_\omega \mathcal{A}\mathcal{P}\sigma \cdot \mathcal{P}\sigma dx$ *where* $\mathcal{A}$ *is an ad hoc tensor. If we want to design mechanisms, we can also introduce a target* σ_0 *and minimize* $J^*(\theta, m_i) = \int_\Omega \chi_\omega \left(|\mathcal{P}\sigma|^2 - 2\sigma_0 \cdot \sigma + |\sigma_0|^2\right) dx$.

The Young modulus E_B of material B is normalized to 1 and its Poisson ratio is fixed to 0.3. The Young modulus E_A of the weak material A is taken equal to 10^{-2} (with the same Poisson ratio 0.3). The algorithm is initialized with a density $\theta_0(x)$. Usually, we start with a constant uniform value of θ_0. This is the case for the medium cantilever displayed on Figure 4 where the fixed overall volume fraction of material B is 30% and where the number of laminations is $q = 7$ and $\omega = \Omega$. For the same problem, we started from a non-uniform density $\theta_0(x)$ which was optimal

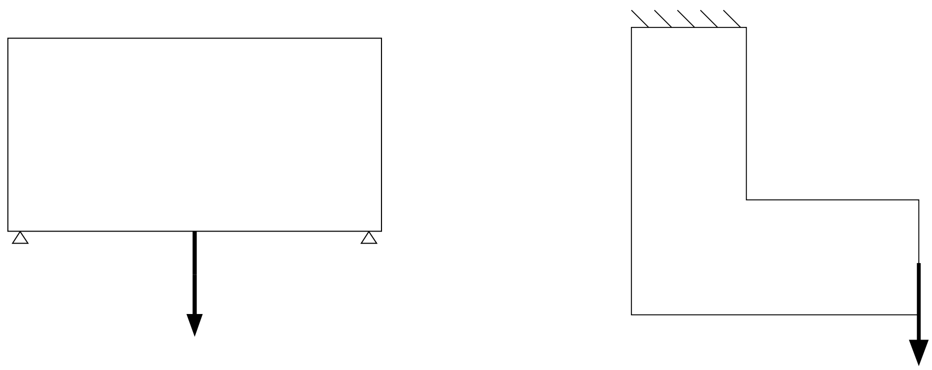

FIG. 2 – Boundary conditions for the arch (left) and the L-beam (right) problems.

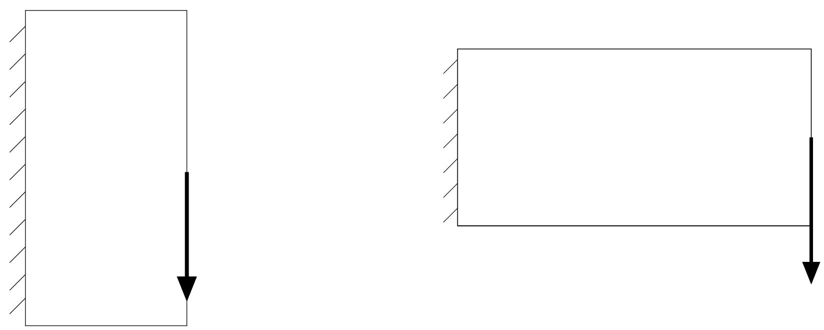

FIG. 3 – Boundary conditions for the short (left) and the medium (right) cantilever problems.

for the compliance minimization. The number of laminations is still $q = 7$, the volume fraction of material B is 30% and $\omega = \Omega$. Both shapes in Figure 5 look similar, but the objective function has decreased (see Figure 6) which proves that the optimal shape is not the same for compliance or stress minimization. Remark also that the optimal shapes in Figures 4 and 5 (right) are the same although they correspond to two different initializations.

When we increase the number of laminations for the same cantilever problem, one clearly get a nicer shape which contains more composite (compare Figure 4 with $q = 7$ and Figure 7 (right) with $q = 23$). On the other hand, if we fix the values of the $(m_i = 1/7)_{1 \leq i \leq 7}$ and optimize only with respect to the density θ, we obtain an optimal shape with much less composite zones (see Figure 7 left).

The same phenomenon can be reproduced on an arch problem (see Figures 8 and 9). One can check on Figure 10 that the optimality of the composite shape increases with the number q of laminations, although the minimum value of J^* does not change too much from $q = 9$ to $q = 36$.

We now investigate the influence of the choice of the localization zone ω in the objective function (30). We study the arch problem with three different choices of ω which localizes j either in a

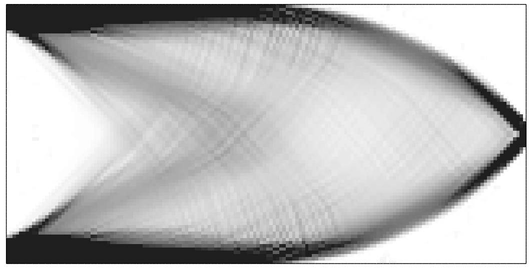

FIG. 4 – Medium cantilever : optimal design for stress minimization starting from a uniform density $\theta_0 = 0.3$ and $\omega = \Omega$. $q = 7$.

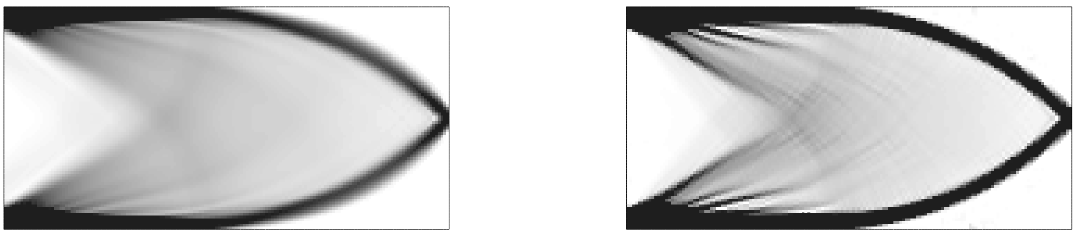

FIG. 5 – Medium cantilever : optimal design (right) for stress minimization starting from a density θ_0 which was optimal for compliance minimization (left), with $q = 7$ and $\omega = \Omega$.

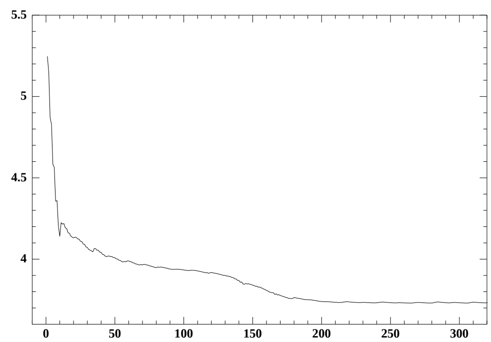

FIG. 6 – Convergence history of the medium cantilever when starting from the optimal design for compliance minimization (see Figure 5).

neighbourhood of the high stress zone or far from it (see Figures 11, 12, 13). Surprisingly, the size, topology and localization of ω do not seem to be relevant parameters in the capture of the optimal shape. This is due to the fact that instead of true void we have a weak elastic phase A ($E_A = 10^{-4}$ in our simulations except in the case of Figure 8) as is usual in the homogenization method. For minimum stress design this approximation seems to be questionable (although it is

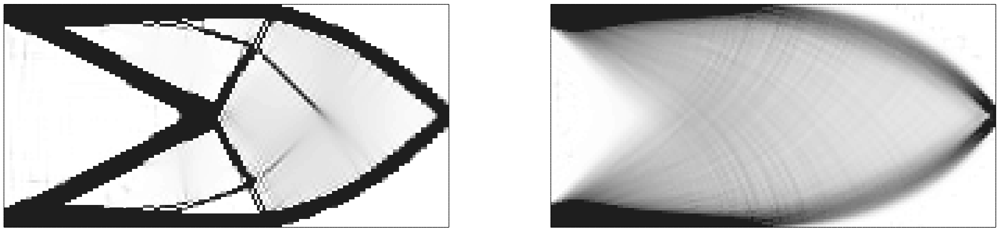

FIG. 7 – Medium cantilever : optimal design for $q = 23$ (right), and for fixed (m_i) with $q = 7$, optimizing only with respect to θ (left). In both cases, $\theta_0 = 0.3$ and $\omega = \Omega$.

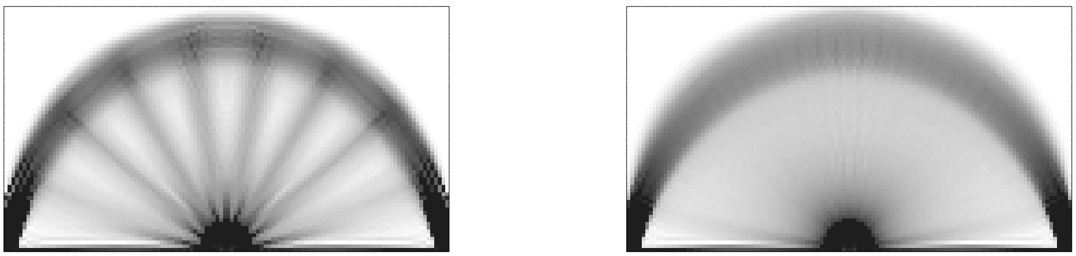

FIG. 8 – The arch : optimal design with $q = 9$ (left) and $q = 36$ (right). In both cases, $\theta_0 = 0.3$ and $\omega = \Omega$.

rigorously proved to be consistent for compliance minimization, see [1], [4]). For example, in the case of Figure 13, if A was true void, an optimal solution would be obtained by any shape that does not intersect the black squares (the stress would be zero in these squares, thus yielding a minimal zero value for the objective function). Instead we obtain a different optimal composite shape which is stable when decreasing the Young modulus of A (see Figure 14). The point is that in a weak phase (however weak it may be) the stress is never zero as in void, and thus the structure should be optimized to minimize it.

Remark that we may decide that ω is not subject to optimization and is, for instance, always

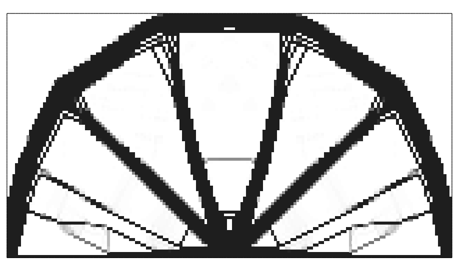

FIG. 9 – The arch : optimal design when optimizing only with respect to θ with fixed (m_i), $q = 3$, $\theta_0 = 0.3$ and $\omega = \Omega$.

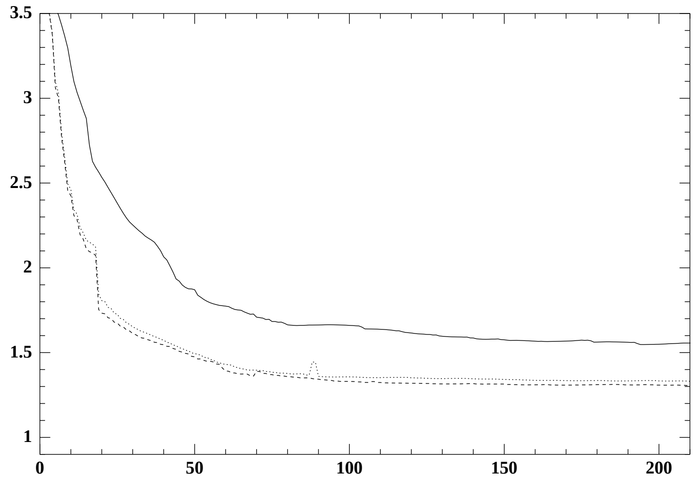

FIG. 10 – The arch : convergence history when $q = 36$ (- - -), $q = 9$ (...) or when optimizing with respect to θ only with fixed (m_i) and $q = 3$ (—). In all cases, $\theta_0 = 0.3$ and $\omega = \Omega$.

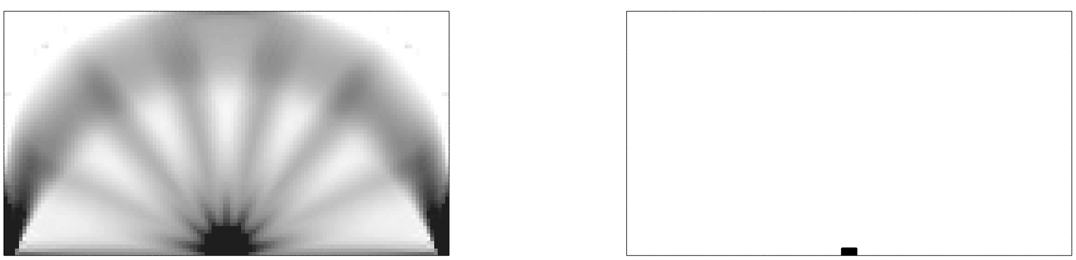

FIG. 11 – The arch : optimal design with $q = 7$, $\theta_0 = 0.3$. The subset ω is the black zone on the right.

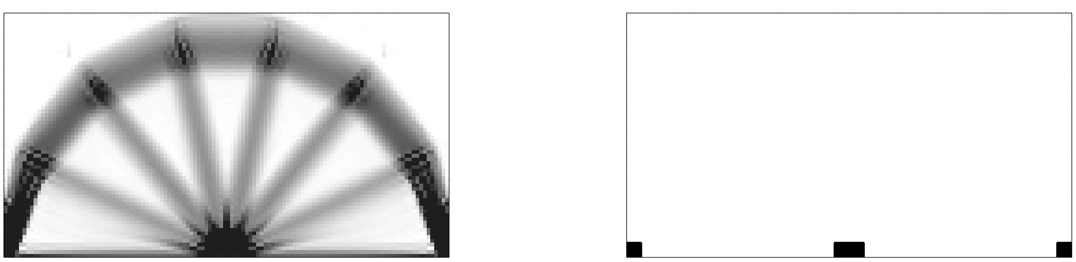

FIG. 12 – The arch : optimal design with $q = 7$, $\theta_0 = 0.3$. The subset ω is the black zone on the right.

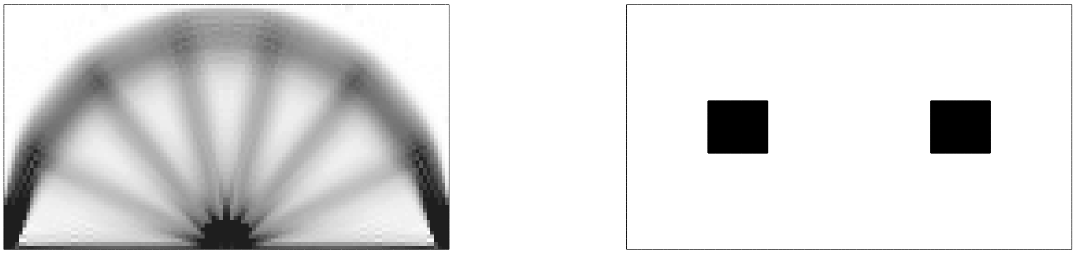

FIG. 13 – The arch : Optimal design with $q = 7$, $\theta_0 = 0.3$. The subset ω is the black zone on the right.

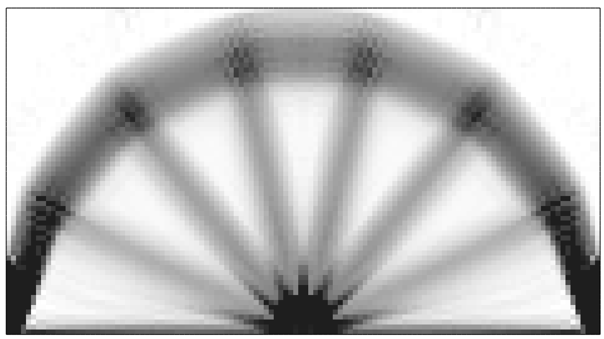

FIG. 14 – The arch : optimal design with $q = 7$, $\theta_0 = 0.3$, and the same subset ω as in Figure 13. The weak phase is weaker : $E_A = 10^{-5}$.

filled with the strong material B. Then j does not explicitly (but only implicitly through u) depend on the design variables θ and (m_i), i.e. $\frac{\partial j}{\partial \theta} = \frac{\partial j}{\partial m_i} = 0$ in (29). In this case, the minimization of J^* (and the optimization of A^*) only relies on the adjoint state contribution which is enough to recover an optimal composite shape. This is the case, for example, in Figure 11 where the same optimal shape is obtained if ω is filled with the strong material B which can not be removed during the optimization process.

Another example is the L-beam (see Figure 15). Remark that there is a stress concentration at the re-entrant corner and that our algorithm is unable to change the shape of the corner in order to reduce this stress concentration (whatever the choice of ω is).

Finally we observe that the optimal short cantilever does not *exactly* correspond to the classical orthogonal two bar truss design which is optimal for compliance minimization (see Figures 16 and 17 for different working domains, design variables and volume of phase B).

All the results presented here are optimal *composite* shapes, i.e. there was no penalization of intermediate densities in order to obtain a *classical* shape (black and white design). As a matter of fact, the traditional penalization procedures, which act on the density θ by forcing it to be close to 0 or 1, do not work so well in practice on stress minimization problems. Rather, we advocate

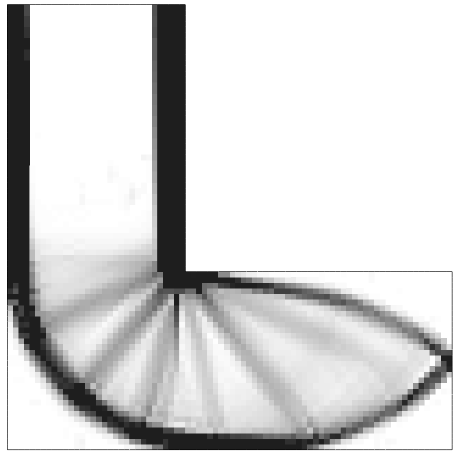

FIG. 15 – L-beam : optimal composite shape. $q = 7$, $\theta_0 = 0.3$ and $\omega = \Omega$.

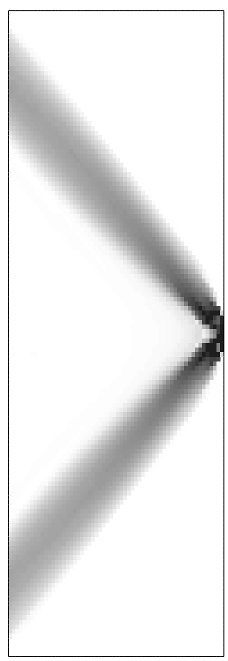

FIG. 16 – Short cantilever : optimal design. $q = 7$, $\theta_0 = 0.1$ and $\omega = \Omega$.

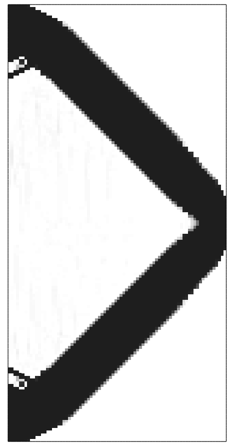

FIG. 17 – Short cantilever : optimal design when optimizing with respect to θ only with fixed (m_i). $q = 7$, $\theta_0 = 0.3$ and $\omega = \Omega$.

a different penalization scheme which relies on microstructure reduction : after convergence to a composite optimal design, we reduce the number of laminations or we fix arbitrarily the values of the lamination parameters. This has the effect of penalizing intermediate densities as is clear from the results of Figures 7 (left), 9, 17, where only the density θ was subject to optimization.

Références

[1] Allaire, G., *Shape optimization by the homogenization method*, Springer Verlag, New York (2001).

[2] Allaire, G., Aubry, S., Jouve, F., Shape optimization with general objective functions using partial relaxation, *in Topology optimization of structures and composite continua, G.I.N. Rozvany and N. Olhoff eds.*, pp.239-249, Kluwer Academic Publishers (2000).

[3] Allaire, G., Aubry, S., Jouve, F., Eigenfrequency optimization in optimal design, *Comp. Meth. App. Mech. Engrg.* 190, pp.3565-3579 (2001).

[4] Allaire, G., Bonnetier, E., Francfort, G.,Jouve, F., Shape optimization by the homogenization method, *Nümerische Mathematik* **76**, 27-68 (1997) .

[5] Allaire, G., Jouve F., Optimal design of micro-mechanisms by the homogenization method, *European Journal of Finite Elements*, 11, pp.405-416 (2002).

[6] Allaire, G., Kohn, R.V., Optimal design for minimum weight and compliance in plane stress using extremal microstructures, *Europ. J. Mech. A/Solids* **12**, 6, 839-878 (1993).

[7] Bendsoe, M., *Methods for optimization of structural topology, shape and material,* Springer Verlag, New York (1995).

[8] Bendsoe, M., Kikuchi, N., Generating Optimal Topologies in Structural Design Using a Homogenization Method, *Comp. Meth. Appl. Mech. Eng.* **71**, 197-224 (1988).

[9] Bendsoe M., Sigmund O., Material interpolation schemes in topology optimization, *Arch. Appl. Mech.* 69, pp.635-654 (1999).

[10] Bendsoe M., Sigmund O., *Topology Optimization. Theory, Methods, and Applications*, Springer Verlag, New York (2003).

[11] Briane, M., Correctors for the homogenization of a laminate, *Advances in Mathematical Sciences and Applications*, Gakkotosho, Tokyo, **4**, 357-379 (1994).

[12] Cherkaev A., *Variational Methods for Structural Optimization,* Springer Verlag, New York (2000).

[13] Cherkaev A., Kohn R.V., Editors, *Topics in the mathematical modeling of composite materials,* Progress in Nonlinear Differential Equations and their Applications, 31, Birkhaüser, Boston (1997).

[14] Duysinx, P., Bendsoe, M., Topology Optimization of Continuum Structures with Local Stress Constraints, *Int. J. Num. Meth. Engng.*, 43, pp.1453-1478 (1998).

[15] Grabovsky, Y., Optimal design problems for two-phase conducting composites with weakly discontinuous objective functionals, *Adv. in Appl. Math.*, 27, pp.683-704 (2001).

[16] Kohn, R.V., Strang, G., Optimal Design and Relaxation of Variational Problems I-II-III, *Comm. Pure Appl. Math.* **39**, 113-137, 139-182, 353-377 (1986).

[17] Lipton, R., Design of functionally graded composite structures in the presence of stress constraints, *Int. J. Solids Structures*, 39, pp.2575-2586 (2002).

[18] Lipton, R., Velo, A., Optimal design of gradient fields with applications to electrostatics, *Nonlinear partial differential equations and applications, Séminaire du Collège de France*, Vol. XIV (Paris, 1997/1998), pp.509–532, Stud. Math. Appl., 31, North-Holland, Amsterdam (2002).

[19] Lurie, K., Cherkaev, A., Effective characteristics of composite materials and the optimal design of structural elements, *Uspekhi Mekhaniki* **9**, 3-81 (1986). English translation in [13].

[20] Milton, G., *The theory of composites,* Cambridge University Press (2001).

[21] Murat, F., Tartar, L., H-convergence, *Séminaire d'Analyse Fonctionnelle et Numérique de l'Université d'Alger*, mimeographed notes (1978). English translation in [13].

[22] Murat, F., Tartar, L., Calcul des Variations et Homogénéisation, in D. Bergman et. al. (eds.), *Les Méthodes de l'Homogénéisation Théorie et Applications en Physique*, Coll. Dir. Etudes et Recherches EDF, **57**, Eyrolles, Paris, pp.319-369 (1985). English translation in [13].

[23] Meyers N.G., An L^p-estimate for the gradient of solutions of second-order elliptic divergence equations, *Ann. Sc. Norm. Sup. Pisa* **17**, pp.198-206 (1963).

[24] Pedregal, P., Fully explicit quasiconvexification of the mean-square deviation of the gradient of the state in optimal design, *Electr. Res. Announc. of the A.M.S.*, 7, pp.72-78 (2001).

[25] Rozvany, G., Bendsoe, M., Kirsch, U. Layout optimization of structures, *Appl. Mech. Reviews* **48**, 41-118 (1995).

[26] Tartar, L., Remarks on optimal design problems, *in Calculus of variations, homogenization and continuum mechanics, G. Bouchitté et al. eds.*, Series on Adv. in Math. for Appl. Sci, 18, pp.279-296, World Scientific, Singapore (1994).

[27] Zhou M., Rozvany G., The COC algorithm, Part II : Topological, geometrical and generalized shape optimization, *Comp. Meth. App. Mech. Engrg.* 89, pp.309-336 (1991).